Relativistic mean field approach with density dependent couplings for finite nuclei

H. Shen,[1,3] Y. Sugahara,[2] and H. Toki[1,2]
[1]*Research Center for Nuclear Physics (RCNP), Osaka University, Ibaraki, Osaka 567, Japan*
[2]*The Institute of Physical and Chemical Research (RIKEN), Hirosawa, Wako, Saitama 351, Japan*
[3]*Department of Physics, Nankai University, Tianjin 300071, China*
(Received 9 August 1996)

We study finite nuclei within the relativistic mean field approach with density dependent couplings (RMFD) based on the relativistic Brueckner-Hartree-Fock (RBHF) results on nuclear matter. We take the linear relativistic mean-field Lagrangian with mesons σ, ω, δ, and ρ, whose coupling constants with nucleons are determined so as to reproduce the RBHF results of nuclear matter at various densities and proton fractions. We apply the RMFD approach to various nuclei with spherical shape including unstable ones in the periodic table. We find satisfactory results on the nuclear properties. We emphasize here that the proton and neutron effective masses are largely different from each other as the proton fraction is decreased from $Y_p=0.5$, which forces us to include the isovector scalar meson δ in our approach. [S0556-2813(97)00703-6]

PACS number(s): 21.60.Jz, 21.65.+f

I. INTRODUCTION

It is very important to reproduce the saturation property of nuclear matter for the description of finite nuclei and also of neutron stars and supernovas. The long efforts with the Brueckner theory in the nonrelativistic framework revealed that the use of the two-body interaction extracted from the nucleon-nucleon scattering does not reproduce the saturation property [1]. The calculated results with various tensor strengths on the saturation point rather fall in the so-called Coester line, which tends to avoid the empirical saturation point [2].

Recently, Brockmann and Machleidt took the relativistic framework and performed the relativistic Brueckner Hartree-Fock (RBHF) calculation, where the coupling constants and the form factors of the one-boson exchange potential (OBEP) were fixed by the nucleon-nucleon scattering data [3]. They found that the relativistic description was essential and provided a new Coester line, which goes through near the empirical saturation point. In particular, the use of the parameter set A, which has the smallest tensor strength among the parameter sets used there, reproduces nearly the saturation property [3]. The relativistic effect provides a strong density-dependent repulsion, which changes the equation of state (EOS) totally at higher densities than that of the nonrelativistic EOS [4,5]. This density-dependent repulsion originates from the pair term (Z graph), if expressed in the nonrelativistic language [4,5].

Encouraged by this finding, there were many applications of the RBHF results on nuclei and neutron stars. The RDDH approach was developed for finite nuclei with the use of the relativistic mean-field (RMF) theory with density-dependent couplings so as to reproduce the RBHF results [6]. This RDDH approach provided very good results on the nuclear properties as the binding energy and the nuclear radii for ^{16}O and ^{40}Ca. Including the ρ meson and the rearrangement terms, finite nuclei including heavy ones are studied in the same framework [7]. Applications were done also for neutron stars [8,9]. The calculations of Brockmann and Machleidt were, however, limited to nuclear matte and neutron matter [3].

Very recently, Engvik *et al.* calculated the matter properties at various densities by changing the proton fractions [10]. They applied the RBHF results to neutron stars by imposing the β equilibrium condition. With their efforts, we now have new information on the behavior of nuclear matter at various proton fractions. A thorough investigation of the RBHF result is very important for the understanding of nuclear matter properties. It is then very interesting to apply the RBHF results on finite nuclei, as was done for symmetric nuclei.

Hence, in this paper, we would like to develop the relativistic mean-field theory with variable coupling constants (RMFD) so as to reproduce the RBHF results at various proton fractions. We would then apply the RMFD approach to nuclei in the periodic table.

This paper is arranged as follows. In Sec. II, we briefly discuss the RMFD approach and the method of fixing the coupling constants using the RBHF results. In Sec. III, we present the behavior of nuclear matter at various densities and proton fractions. We show also the behaviors of the coupling constants extracted from the RBHF results. We then apply the RMFD approach to finite nuclei and compare the results with experimental data for many nuclei including some unstable nuclei in Sec. IV. We devote Sec. V to the summary of the present work.

II. RMFD APPROACH

We follow exactly the concept of the RDDH approach for the construction of the RMFD method [6]. The concept is similar to the work of Negele for his application of the nonrelativistic Brueckner-Hartree-Fock results on finite nuclei using the local density approximation [11].

We start with the RMF Lagrangian [12,13],

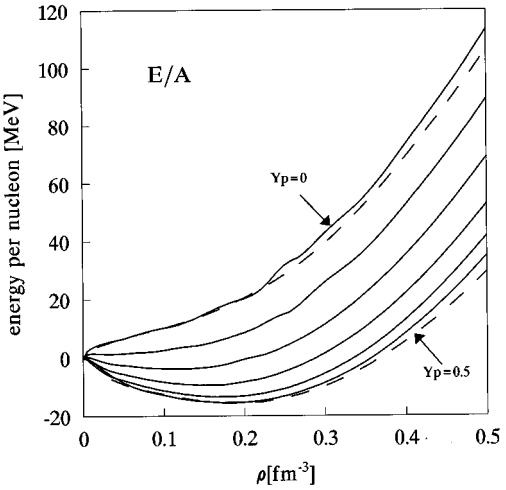

FIG. 1. Energy per particle E/A of nuclear matter for various proton fractions Y_p as a function of the nuclear matter density ρ. The solid curves denote the results of Engvik in steps of $\Delta Y_p=0.1$ starting from $Y_p=0.5$ to $Y_p=0$. The results of Brockmann and Machleidt for $Y_p=0.5$ and $Y_p=0$ are shown by dashed curves, for comparison.

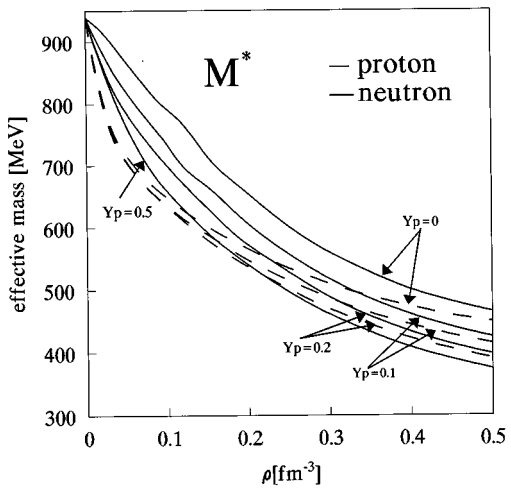

FIG. 2. Effective masses for protons and neutrons for various proton fractions ($Y_p=0.5$, 0.2, 0.1, and 0) as a function of nuclear matter density ρ. These are the results of Engvik using the RBHF theory.

$$L_{\mathrm{RMFD}}=\bar{\psi}\Big[i\gamma_\mu\partial^\mu-M-g_\sigma(\rho)\sigma-g_\omega(\rho)\gamma_\mu\omega^\mu-g_\delta(\rho)\tau^a\delta^a-g_\rho(\rho)\tau^a\gamma_\mu\rho^{a\mu}-e\,\frac{(1-\tau^a)}{2}\,\gamma_\mu A^\mu\Big]\psi+L_B. \quad (1)$$

Here, we have explicitly written the density dependence of the coupling constants g_σ, g_ω, g_δ, g_ρ. Hence, we write RMFD as the suffix of the Lagrangian, where D stands for density. Although written here is only ρ, we mean it as ρ_p and ρ_n, the proton and the neutron densities. ψ denotes the nucleon field including protons and neutrons with M being their mass and γ_μ the Dirac γ matrix. τ^a is the isospin matrix; the Pauli matrix, with the eigenvalues for τ^3, are $+1$ for neutrons and -1 for protons in our nuclear physics convention. In addition to the σ, ω, and ρ mesons, we have introduced the isovector scalar meson δ, which is found necessary to reproducing the results of RBHF for various ρ_p and ρ_n. L_B denotes the boson Klein-Gordon part in the standard form [12,13]. A^μ denotes the electromagnetic (EM) photon field with the electric charge e. This Lagrangian is to be considered as that in the nuclear matter frame of the Lorentz invariant expression of the RMFD Lagrangian [7].

In order to make a connection with the results of RBHF at various ρ_p and ρ_n, we first work out infinite matter. We take the mean-field approximation for the meson and the photon fields and all the symmetry requirements. For general ρ_p and ρ_n, we get the Dirac equation

$$[i\gamma_\mu\partial^\mu-M-g_\sigma(\rho)\sigma-g_\omega(\rho)\gamma_0\omega^0-g_\delta(\rho)\tau^0\delta^0-g_\rho(\rho)\tau^0\gamma_0\rho^{00}]\psi=0 \quad (2)$$

with

$$\sigma=-\frac{g_\sigma(\rho)}{m_\sigma^2}(\rho_s^n+\rho_s^p),$$

$$\omega^0=+\frac{g_\omega(\rho)}{m_\omega^2}(\rho_\nu^n+\rho_\nu^p),$$

$$\delta^0=+\frac{g_\delta(\rho)}{m_\delta^2}(\rho_s^n-\rho_s^p), \quad (3)$$

$$\rho^{00}=-\frac{g_\rho(\rho)}{m_\rho^2}(\rho_\nu^n-\rho_\nu^p).$$

The ρ_s's are the scalar densities,

$$\rho_s^n=2\int_0^{k_f^n}\frac{d^3k}{(2\pi)^3}\frac{M_n^*}{E_n^*} \quad (4)$$

and the corresponding one for ρ_s^p. Here, the effective mass M_n^* is given as $M_n^*=M+g_\sigma(\rho)\sigma+g_\delta(\rho)\delta^0$ for neutron and $M_p^*=M+g_\sigma(\rho)\sigma-g_\delta(\rho)\delta^0$ for proton. The energies are $E_n^2=k^2+M_n^{*2}$ and $E_\rho^2=k^2+M_p^{*2}$. The ρ_v's are the vector densities,

$$\rho_\nu^n=2\int_0^{k_f^n}\frac{d^3k}{(2\pi)^3}, \quad (5)$$

and the corresponding one for ρ_ν^p. We note that we have dropped the rearrangement contribution in the Dirac equation, since such a consideration is not made in the RBHF calculation [7].

The RBHF calculation provides U_s^n, U_s^p, U_ν^n, and U_ν^p for various ρ_p and ρ_n. These scalar and vector potentials are related with the coupling constants as

$$
\begin{aligned}
U_s^n + U_s^p &= -\frac{2g_\sigma^2(\rho)}{m_\sigma^2}(\rho_s^n + \rho_s^p),\\
U_\nu^n + U_\nu^p &= +\frac{2g_\omega^2(\rho)}{m_\omega^2}(\rho_\nu^n + \rho_\nu^p),\\
U_s^n - U_s^p &= +\frac{2g_\delta^2(\rho)}{m_\delta^2}(\rho_s^n - \rho_s^p),\\
U_\nu^n - U_\nu^p &= -\frac{2g_\rho^2(\rho)}{m_\rho^2}(\rho_\nu^n - \rho_\nu^p).
\end{aligned}
\tag{6}
$$

These relations indicate that the complete reproduction of the RBHF results needs the δ meson. We shall discuss the behaviors of U's and further the extracted g's at various densities in the next section. We mention here that we have used the approximation that the Dirac potentials are momentum independent, although they depend on the densities (Fermi momentum). This approximation is extremely good for nucleons up to slightly above the Fermi momentum [3]. The variation of the potentials with momentum is less than a few percent. This momentum dependence is included in their self-consistent calculations of the RBHF equations [3,10]. Hence the calculated results under this approximation are slightly different from the RBHF results for E/A. The difference is, however, very small.

We write the equations of motion of nucleons and mesons for finite nuclei. The normal modes of the nucleon field are obtained by solving the following equation:

$$
\begin{aligned}
\Big[&-i\boldsymbol{\alpha}\cdot\boldsymbol{\nabla} + \beta M + \beta g_\sigma(\rho)\sigma(r) + g_\omega(\rho)\omega^0(r)\\
&+ \beta g_\delta(\rho)\tau^0\delta^0(r) + g_\rho(\rho)\tau^0\rho^{00}(r) - e\,\frac{(1-\tau^0)}{2}A^0(r)\\
&+ R_n(\rho)\,\frac{1+\tau^0}{2} + R_p(\rho)\,\frac{1-\tau^0}{2}\Big]\psi_i = E_i\psi_i
\end{aligned}
\tag{7}
$$

with the rearrangement term $R_n(\rho)$ for neutrons,

$$
\begin{aligned}
R_n(\rho) = &\left[\frac{\partial}{\partial\rho_n}g_\sigma(\rho)\right]\sigma(r)\langle\overline{\psi}\psi\rangle + \left[\frac{\partial}{\partial\rho_n}g_\omega(\rho)\right]\omega^0(r)\langle\overline{\psi}\gamma^0\psi\rangle\\
&+\left[\frac{\partial}{\partial\rho_n}g_\delta(\rho)\right]\delta^0(r)\langle\overline{\psi}\tau 0\,\psi\rangle + \left[\frac{\partial}{\partial\rho_n}g_\rho(\rho)\right]\rho^{00}(r)\\
&\times\langle\overline{\psi}\tau^0\gamma^0\psi\rangle.
\end{aligned}
\tag{8}
$$

We get a similar expression for $R_p(\rho)$, which is obtained by replacing ρ_n by ρ_p in the derivative of the coupling constants. The Klein-Gordon equations for σ, ω, δ, ρ are

$$
\begin{aligned}
(-\boldsymbol{\nabla}^2 + m_\sigma^2)\sigma(r) &= -g_\sigma(\rho)[\rho_s^n(r) + \rho_s^p(r)],\\
(-\boldsymbol{\nabla}^2 + m_\omega^2)\omega^0(r) &= +g_\omega(\rho)[\rho_\nu^n(r) + \rho_\nu^p(r)],\\
(-\boldsymbol{\nabla}^2 + m_\delta^2)\delta^0(r) &= +g_\delta(\rho)[\rho_s^n(r) - \rho_s^p(r)],\\
(-\boldsymbol{\nabla}^2 + m_\rho^2)\rho^{00}(r) &= -g_\rho(\rho)[\rho_\nu^n(r) - \rho_\nu^p(r)],\\
-\boldsymbol{\nabla}^2 A^0(r) &= e\rho_\nu^p(r).
\end{aligned}
\tag{9}
$$

We solve these coupled differential equations self-consistently. After solving the coupled differential equations, we can calculate all the physical quantities. The expression for the energy is $E = E_0 + E_R$, where

$$
E_R = -\int d^3r[R_n(\rho)\rho_n(r) + R_p(\rho)\rho_p(r)] \tag{10}
$$

is the rearrangement contribution with E_0 being the energy without the rearrangement contribution [12,13]. We remove the center-of-mass contribution using the simplest formula as in Ref. [14]

$$
\Delta E_{\text{c.m.}} = \frac{3}{4}41A^{-1/3}. \tag{11}
$$

We take the pairing correlations into account by using the BCS theory, following the procedure of Refs. [14] and [15]. In this work, we do not consider the deformations.

III. RBHF RESULTS AND THE RMFD PARAMETERS

We present here the results of the RBHF calculations obtained by Engvik *et al.* [10]. First of all, we show in Fig. 1 the energy per particle of nuclear matter for various proton fractions, $Y_p[=\rho_p/(\rho_n+\rho_p)]$, as a function of the nuclear matter density $\rho(=\rho_n+\rho_p)$. The solid curves denote the results of Engvik in step of $\Delta Y_p = 0.1$ starting from $Y_p = 0.5$ to $Y_p = 0$. As comparison, we show the results of Brockmann and Machleidt [3] by dashed curves for $Y_p = 0.5$ (nuclear matter) and $Y_p = 0$ (neutron matter). We note that E/A shown here are calculated by using U_ν and U_s and therefore they are slightly different from the values tabulated in their papers [3,10]. These two groups do the same calculations and should get the same results for $Y_p = 0.5$ and $Y_p = 0$. The differences are not large, but appreciable. They should originate from the ambiguities in extracting U_ν and U_s. U_ν and U_s are, in principle, dependent not only on the Fermi momentum (density), but also on the momentum of each nucleon. They are, however, approximated to be constant of momentum. The slight fluctuations seen in the results of Engvik are to be considered as the numerical ambiguities in extracting U_ν and U_s in the RBHF calculations at present.

Surprising results of the RBHF calculations are shown in Fig. 2 for the proton and the neutron effective masses M^* for various Y_p as a function of nuclear matter density ρ. For $Y_p = 0.5$, the effective masses for protons and neutrons are the same, as indicated by the thick solid curve. As Y_p is decreased, the neutron effective mass increases at all densities, where the cases for $Y_p = 0.2$, 0.1, and 0 are shown consecutively with sold curves to avoid confusion of the presentation. The proton effective mass behaves differently. At

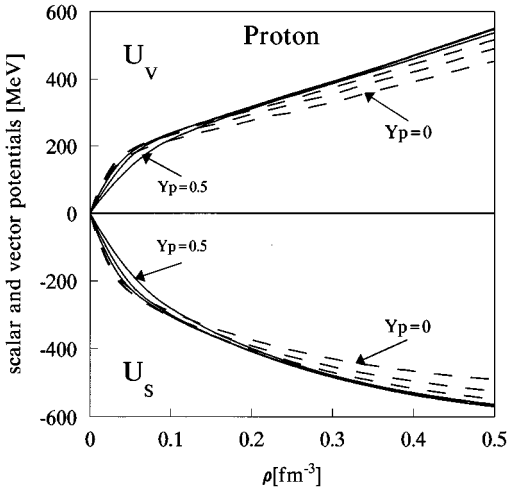

FIG. 3. The scalar and vector potentials for protons for various proton fractions Y_p as a function of the nuclear matter density ρ. The results at $Y_p=0.5$, 0.4, and 0.3 are denoted by solid curves and those at $Y_p=0.2$, 0.1, and 0 by dashed curves. These are the results of Engvik using the RBHF theory.

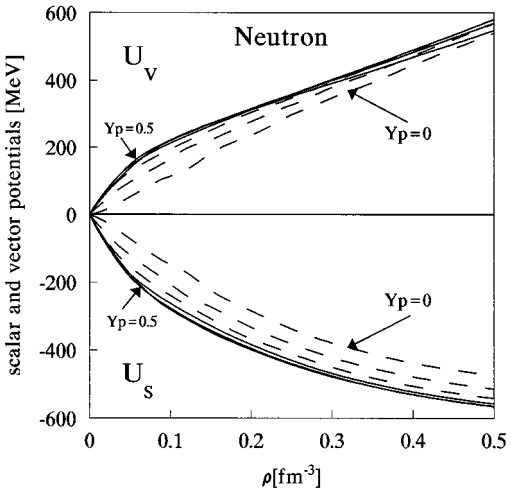

FIG. 4. The scalar and vector potentials for neutrons for various Y_p, as a function of the nuclear matter density ρ. The notations are the same as in Fig. 3.

smaller densities, the proton effective mass decreases with decreasing Y_p, while at larger densities, it increases with Y_p, which is shown by dashed curves. At large ρ, the effective masses of protons and neutrons tend to coincide. This effect is not considered up to now in any of the relativistic mean-field (RMF) theories [14,16].

We also show the results of the RBHF calculations on the vector and the scalar potentials for protons and neutrons at various proton fractions in step of $\Delta Y_p=0.1$ as functions of the nuclear matter density in Figs. 3 and 4. We recognize that the potentials are almost unchanged at large Y_p for $0.3<Y_p<0.5$ as shown by solid curves except for the proton potentials at small densities. However, they change largely as Y_p is decreased further, which is shown by dashed curves. Notice that the behaviors of potentials are largely different between protons and neutrons at small Y_p.

From these vector and scalar potentials for protons and neutrons at various densities and proton fractions, we are able to extract the coupling constants $g_\sigma, g_\omega, g_\delta, g_\rho$. Since the range information is lost in nuclear matter, we take the masses of mesons as those values of the parameter set A. They are $m_\sigma=550$ MeV; $m_\omega=782.6$ MeV; $m_\delta=983$ MeV; $m_\rho=769$ MeV. We consider these masses as our standard choice of the study of finite nuclei. We show in Fig. 5 the coupling constants for various Y_p as a function of the nuclear matter density.

The σ meson coupling g_σ decreases with density monotonically. The dependence on the proton fraction Y_p is interesting. At large ρ ($\rho>0.1$ fm^{-3}), the Y_p dependence is small down to $Y_p\sim0.3$, but it becomes strong for smaller Y_p. At smaller ρ ($\rho<0.1$ fm^{-3}), g_σ increases with decreasing Y_p down to $Y_p\sim0.3$ and then decreases with decreasing Y_p. We note here that the behavior of the calculated results of Engvik at $\rho=0.035$ *and* 0.049 with $Y_p=0.45$ and 0.5 is irregular. On the other hand, such an irregular behavior is not found in the results of Brockmann and Machleidt at $Y_p=0.5$. Therefore, we disregarded the results at these four points. Then we made smooth linear extrapolation using the results at $\rho=0.068$ *and* 0.09 with $Y_p=0.45$ and 0.5 down to $\rho=0$. The same method is used for other coupling constants. We find similar behavior for the ω meson coupling also.

Here, we note that we are unable to drop the Y_p dependence in g_σ and g_ω. In fact, we tried to take out the Y_p dependence of g_σ and g_ω and try to reproduce the RBHF results by using again the Y_p independent isovectors g_δ and g_ρ. The outcome was very bad. Hence, we decided to allow the Y_p dependence for all the couplings.

The δ meson coupling g_δ decreases monotonically with density. The Y_p dependence seems weak. Hence, for our practical study of finite nuclei, we may be able to take Y_p independent g_δ. This observation is true also for g_ρ. In this study, however, we keep the small Y_p dependence for calculations of finite nuclei.

The ρ meson coupling g_ρ also decreases monotonically with density. At high density ($\rho>0.2$ fm^{-3}), it even changes sign. We need to explain this sign change of g_ρ. In the RMF theory, we change the sign of the meson Lagrangian entirely for the ρ meson, the kinetic part, and the mass part, in order to change the repulsive contribution of the ρ meson to the attractive contribution. This change of the sign of the ρ meson part does not influence the results of finite nuclei, since the nuclear density does not go up to this large value.

IV. FINITE NUCLEI

We calculate finite nuclei with the RMFD approach. The parameters for the meson couplings are those shown in Fig. 5. The calculated results for the binding energy per particle BE/A and the charge radius R_c are compared with experiment in Table I. In addition to stable nuclei, we calculate also unstable nuclei in order to see the isovector effect.

The experimental values are listed in the second column in units of MeV. When we choose the standard masses for mesons, the results found are those listed in the third column. The energy is about 1 MeV smaller (under binding) for ^{16}O. The corresponding charge radius is 2.61 fm as compared to the experimental value 2.74 fm, as listed in the seventh and sixth columns. The radius is about 0.1 fm smaller than ex-

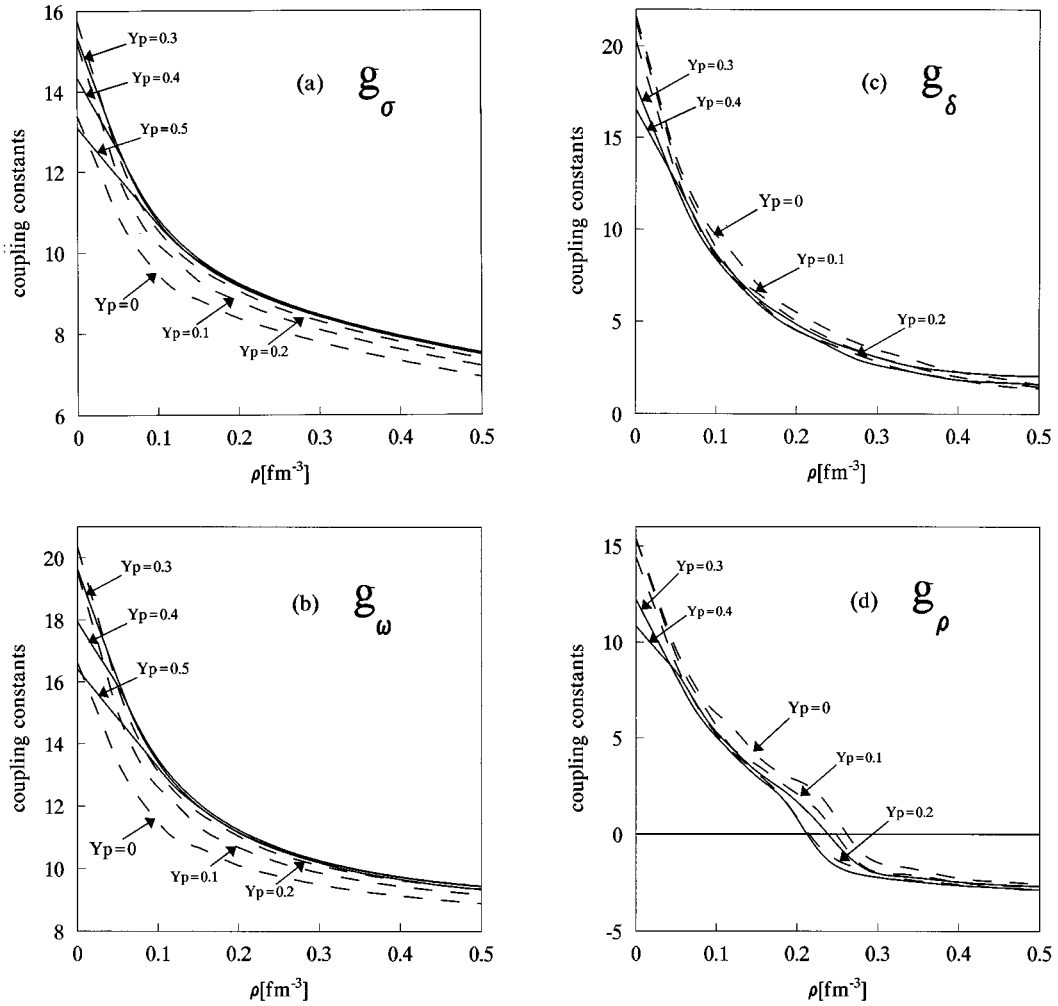

FIG. 5. The coupling constants, g_σ, g_ω, g_δ, and g_ρ, for various proton fractions Y_p as a function of the nuclear matter density ρ. The standard masses are used for these mesons, m_σ=550 MeV; m_ω=782.6 MeV; m_δ=983 MeV; m_ρ=769 MeV in order to extract the coupling constants from the scalar and the vector potentials of Engvik. The results at Y_p=0.5, 0.4, and 0.3 are denoted by solid curves and those at Y_p=0.2, 0.1, and 0 by dashed curves. (a) The σ nucleon coupling constant g_σ. (b) The ω nucleon coupling constant g_ω. (c) The δ nucleon coupling constant g_δ. (d) The ρ nucleon coupling constant g_ρ.

periment. This small radius is related with the saturation density of the RBHF results with set A, which is 0.19 fm^{-3} instead of 0.17 fm^{-3}. Similar results are also found for ^{40}Ca. Hence, the isoscalar part of the RMFD approach is almost satisfactory.

Here, we would like to make a comparison with the results of Brockmann and Toki [6]. They found the binding energy 7.5 MeV and the charge radius 2.66 fm for ^{16}O and 8.0 MeV and 3.36 fm for ^{40}Ca. These differences are caused by the very small differences in E/A (U_s and U_v) at small density between the two groups [6,10]. In fact, the binding energy result is sensitive to the couplings of g_σ and g_ω at small density. When we replace g_σ and g_ω of Brockmann and Toki, which are based on the RBHF calculation of Brockmann and Machleidt, by the present g_σ and g_ω, at the small density ($\rho<0.04$ fm^{-3}), we found that the binding energy for ^{16}O is decreased by 0.4 MeV and the charge radius decreased by 0.05 fm. We note that the rearrangement term contributions are included in Table I, while they are not included in the results of Brockmann and Toki. These very small differences in E/A (U_s and U_v) at small density by the two groups indicate the difficulty of extracting the momentum independent vector and scalar potentials in the RBHF calculations of nuclear matter.

We should mention also the difference of our results from those of Fuchs *et al.* [7]. They are again based on the RBHF calculation of Brockmann and Machleidt [3]. Hence, the same statement as made above holds in this comparison. We should therefore consider that the effective theory as the RMFD approach, which based on the infinite matter results of the RBHF theory, is almost able to reproduce the properties of finite nuclei. We consider $\Delta E\sim1$ MeV, $\Delta R_c\sim0.1$ fm as the error of the RMFD approach.

Nuclei with the neutron number N being different from the proton number Z are calculated for several nuclei. Generally, the binding energies are smaller by almost 1.5 MeV than the experimental values. The isovector mesons contribute repulsively and reduce the binding energy by about 0.5 MeV. This we can see by suppressing the δ and ρ meson contribution in the RMFD calculations, the results of which are shown in the fourth column for BE/A and in the ninth column for R_c. The change in the charge radius is small.

TABLE I. The binding energies per particle, BE/A [MeV], and the charge radii R_c [fm] are listed for various nuclei denoted in the first column. The experimental values are given in the second column for BE/A and in the sixth column for R_c. RMFD denotes the results of the RMFD calculations with the use of the density dependent couplings for σ, ω, δ, and ρ mesons. The rearrangement terms are also included for these calculations. RMFD with σ, ω denotes the results with only the σ and ω mesons with rearrangement terms. RMFD with $R=0$ denotes those with all the mesons but without the rearrangement terms.

Nucleus	BE/A (MeV)	RMFD	RMFD σ,ω	RMFD $R=0$	R_c (fm)	RMFD	RMFD σ,ω	RMFD $R=0$
^{16}O	7.98	7.01	7.01	6.89	2.74	2.61	2.61	2.50
^{22}O	7.36	5.92	6.34	5.74		2.65	2.61	2.56
^{40}Ca	8.55	7.54	7.54	7.43	3.45	3.31	3.31	3.20
^{48}Ca	8.67	7.18	7.39	7.03	3.45	3.35	3.36	3.24
^{90}Zr	8.71	7.38	7.48	7.19	4.26	4.07	4.07	3.98
^{124}Sn	8.47	6.88	7.17	6.76	4.67	4.51	4.51	4.38
^{208}Pb	7.87	6.20	6.56	6.08	5.50	5.33	5.31	5.15
^{214}Pb	7.77	6.05	6.50	5.95		5.32	5.29	5.21

We discuss here the meson mass dependence. The meson mass contributes to the range of the effective interaction. In principle, the ranges of these interactions could change in nuclear medium from those in free space. The results presented up to now are those with the use of the same meson masses as those of the NN interaction. We know that the use of larger m_σ increases the binding energy, while it decreases the nuclear radii [17]. When we take $m_\sigma=600$ MeV instead of $m_\sigma=550$ MeV, we find BE/A is increased by about 1 MeV and the radius is decreased by about 0.1 fm. A change of a similar amount is also seen when we change the ω meson mass. The change of the isovector meson masses in this range is not so effective.

The rearrangement terms contribute favorably to both the binding energies and the charge radii [7]. They make the potential of the nucleon shallower by about 10 MeV in the middle of the nucleus and hence act repulsively to the potential. The wave functions are therefore pushed outwards, which results in the increase of the charge radius. It has an effect of increasing the radius by about 0.1 fm as can be seen by comparing the seventh column with the ninth column. The results without the rearrangement terms are shown in the fifth column for BE/A. Since we have to subtract the rearrangement energies in the total energy, they provide attraction contribution to the binding energy. They increase the binding energies by about 0.1 to 0.2 MeV.

V. CONCLUSION

We have performed calculations of finite nuclei within the RMFD approach, where the RMF framework is used with the meson couplings being density dependent, ρ_p and ρ_n, which are expressed in terms of the nuclear matter density ρ $(=\rho_n+\rho_p)$ and the proton fraction, Y_p $[=\rho_p/(\rho_n+\rho_p)]$. The meson couplings are fixed at various ρ and Y_p so as to reproduce the RBHF results of Engvik [10]. It is very interesting to note that the effective masses for protons and neutrons are largely different at small Y_p. This large difference can only be accommodated by introducing the δ meson (isovector-scalar meson).

We have made calculations of finite nuclei including the unstable ones in the periodic table in order to better see the isovector effect. We have found the agreement with experiment very satisfactory, keeping in mind that the RMFD approach does not include any additional parameters for finite nuclei. Generally, the binding energies per particle for finite nuclei are less by 1 to 1.5 MeV as compared to experiment. The charge radii are smaller by 0.1 to 0.15 fm than the experimental values.

We have found some differences from the results of other groups, who use the nuclear matter RBHF results of Brockmann and Machleidt. The differences are caused by the extraction of U_s and U_v at small densities. We consider $\Delta E\sim1$ MeV and $\Delta R_c\sim0.1$ fm as the errors of the RMFD approach. Hence, we think the results of the RMFD approach are quite satisfactory.

ACKNOWLEDGMENTS

We are grateful for fruitful discussions with K. Sumiyoshi and K. Oyamatsu on the equations of state of nuclear matter in the use of the results of Engvik *et al.* We thank L. Engvik deeply for kindly letting us use their RBHF results and for various useful comments. Hong Shen acknowledges the generous support of JSPS for her stay at RCNP Osaka, which was essential to the present work.

[1] H. A. Bethe, Annu. Rev. Nucl. Phys. **21**, 93 (1971).
[2] F. Coester, S. Cohen, B. D. Day, and C. M. Vincent, Phys. Rev. C **1**, 769 (1970).
[3] R. Brockmann and R. Machleidt, Phys. Rev. C **42**, 1965 (1990).
[4] B. Keistar and R. B. Wiringa, Phys. Lett. B **173**, 5 (1986).
[5] G. E. Brown, W. Weise, G. Baym, and J. Speth, Comments Nucl. Part. Phys. **17**, 39 (1987).
[6] R. Brockmann and H. Toki, Phys. Rev. Lett. **68**, 3408 (1992).

[7] C. Fuchs, H. Lenske, and H. H. Wolter, Phys. Rev. C **52**, 3043 (1995).
[8] K. Sumiyoshi, H. Toki, and R. Brockmann, Phys. Lett. B **276**, 393 (1992).
[9] K. Sumiyoshi, K. Oyamatsu, and H. Toki, Nucl. Phys. **A595**, 327 (1995).
[10] L. Engvik, E. Osnes, M. Hjorth-Jensen, G. Bao, and E. Ǒstgaard (unpublished); O. Elgaroy, L. Engvik, E. Osnes, F. V. De Blasio, M. Hjorth-Jensen, and G. Lazzari, Phys. Rev. Lett. **76**, 1994 (1996); L. Engvik, M. Hjorth-Jensen, E. Osnes, G. Bao, and E. Ostgaard, *ibid.* **73**, 2650 (1994).
[11] J. W. Negele, Phys. Rev. C **1**, 1260 (1970).
[12] J. D. Walecka, Ann. Phys. (N.Y.) **83**, 491 (1974).
[13] B. D. Serot and J. D. Walecka Adv. Nucl. Phys. **16**, 1 (1986).
[14] Y. Sugahara and H. Toki, Nucl. Phys. **A579**, 557 (1994).
[15] P.-G. Reinhard, M. Rufa, J. Maruhn, W. Greiner, and J. Friedrich, Z. Phys. A **323**, 13 (1986).
[16] D. Hirata, H. Toki, T. Watabe, I. Tanihata, and B. V. Carlson, Phys. Rev. C **44**, 1467 (1991).
[17] H. Toki, Y. Sugahara, D. Hirata, B. V. Carlson, and I. Tanihata, Nucl. Phys. **A524**, 633 (1991).